

Geophysical Research Letters



RESEARCH LETTER

10.1029/2021GL093259

Key Points:

- Tropical cyclones (TCs) that intensify tend to receive greater radiative heating from clouds prior to intensification
- Radiative heating within the TC area creates positive feedbacks to strengthen TC intensity
- Removing cloud-radiative interactions in numerical models slows or inhibits tropical cyclogenesis

Supporting Information:

Supporting Information may be found in the online version of this article.

Correspondence to:

S.-N. Wu,
swu@ou.edu

Citation:

Wu, S.-N., Soden, B. J., & Nolan, D. S. (2021). Examining the role of cloud radiative interactions in tropical cyclone development using satellite measurements and WRF simulations. *Geophysical Research Letters*, 48, e2021GL093259. <https://doi.org/10.1029/2021GL093259>

Received 9 MAR 2021

Accepted 21 JUL 2021

Examining the Role of Cloud Radiative Interactions in Tropical Cyclone Development Using Satellite Measurements and WRF Simulations

S.-N. Wu^{1,2} , B. J. Soden² , and D. S. Nolan²

¹School of Meteorology, University of Oklahoma, Norman, OK, USA, ²Rosenstiel School of Marine and Atmospheric Science, University of Miami, Miami, FL, USA

Abstract This study examines the role of cloud-radiative interactions in the development of tropical cyclones using satellite measurements and model simulations. Previous modeling studies have found that the enhanced cloud radiative heating from longwave radiation in the convective region plays a key role in promoting the development of tropical convective systems. Here, we use satellite measurements and Weather Research and Forecasting Model (WRF) simulations to further investigate how critical cloud radiative interactions are to the development of tropical cyclones (TCs). Clouds and the Earth's Radiant Energy System measurements show that intensifying TCs have greater radiative heating from clouds within the TC area than weakening ones. Based on this result, idealized WRF simulations are performed to examine the importance of the enhanced radiative heating to TC intensification. Sensitivity experiments demonstrate that removing cloud-radiative interactions often inhibits tropical cyclogenesis, suggesting that cloud-radiative interactions play a critical role.

Plain Language Summary It is difficult to accurately predict tropical cyclone (TC) formation. To better understand TC formation, we analyzed the relationship between energy from infrared radiation and TC formation through satellite observations and computer simulations. It was found that TCs with a greater amount of radiative heating from clouds are more likely to intensify over the next few days. Moreover, the probability of TC formation will decrease if the interaction between clouds and radiative heating is blocked. This result suggests that understanding how radiative heating strengthens TCs may improve the performance of hurricane forecasting.

1. Introduction

The prediction of tropical cyclones (TCs) has steadily improved over the past two decades due to advances in numerical models and observing systems (DeMaria et al., 2014; Simon et al., 2018). However, the predictive skill is low when the intensity of TCs is weak, because the evolution of a weak tropical convective system can be more sensitive to the impact from internal dynamical and environmental influences (Cossuth et al., 2013). To better understand the processes responsible for the development of weak TCs, we investigate the energy sources in developing TCs using satellite observations and model simulations.

TCs develop from tropical disturbances (TDs) under situations where the energy supplied to the storm is greater than that dissipated. Recent studies using CloudSat measurements of ice water content found that developing TCs have greater cloud ice water content within 500 km of the TC center than weakening TCs, confirming the importance of latent heating to TC development (Wu & Soden, 2017; Wu et al., 2020, 2021). However, latent heating is important to TCs only when it occurs within ~100 km of the TC center (Nolan, Rappin, & Emanuel, 2007). In addition, latent heating in the early stage of TCs is often too weak and sporadic to support the development of TCs. Thus, during the early stage of TCs, an additional energy source other than latent heating may be required.

Previous theoretical and modeling studies have suggested that radiative heating from clouds may be a crucial energy source for the development of tropical convective systems at their early stage (Bretherton et al., 2005; Dudhia, 1989; Miller & Frank, 1993; Muller & Held, 2012; Wing & Emanuel, 2014; Wing et al., 2017; Xu & Randall, 1995). That is, clouds can alter the spatial distribution of radiative heating, and subsequently change the cloud and precipitation fields through changes in the overturning circulation.

© 2021. The Authors.

This is an open access article under the terms of the [Creative Commons Attribution-NonCommercial License](https://creativecommons.org/licenses/by/4.0/), which permits use, distribution and reproduction in any medium, provided the original work is properly cited and is not used for commercial purposes.

This process transports moist static energy (MSE) into the cloudy area, nurturing a convective system. Such interactions between clouds and radiation create a positive feedback, aggregating energy to facilitate the development of weak tropical convective systems. Therefore, this positive feedback involving cloud-radiative interactions may play an important role in bolstering TC development.

Recent modeling studies have found that radiative fluxes can profoundly influence TC development. Removing cloud-radiative heating often inhibits TC genesis, suggesting that radiative fluxes may play a critical role in the development of Tropical Depressions (Bretherton et al., 2005; Bu et al., 2014; Carstens & Wing, 2020; Dunion et al., 2014; Fovell et al., 2016; Melhauser & Zhang, 2014; Muller & Romps, 2018; Nolan, Moon, & Stern, 2007; Ruppert et al., 2020; Smith et al., 2020; Wing et al., 2016; Wang et al., 2019; Zhang et al., 2021). Radiative feedbacks may assist the initiation of TC genesis by enhancing the circulation that transports energy into the moist convective regions (Muller & Romps, 2018; Wing et al., 2016). In addition, radiative heating may strengthen thermally direct secondary circulation of TCs to accelerate their tangential wind (Ruppert et al., 2020). Although these modeling studies have demonstrated the importance of radiative heating to TC development, observational verification is missing and more idealized simulations with realistic environmental forcings are required to understand the potential influence of the large-scale environment.

This study presents an observational analysis of the relationship between radiative heating from clouds and TC genesis in conjunction with idealized modeling studies to better understand their role in TC development. To achieve these goals, we use satellite measurements from CloudSat and Clouds and the Earth's Radiant Energy System (CERES) to document the relationship of atmospheric radiative heating with TC genesis and intensification. We also use the Weather Research and Forecasting (WRF) model to further examine the importance of radiative processes in the development of TCs using a range of modeling conditions. A MSE framework is used to examine the contribution of radiative fluxes to the increased energy in TCs to further elucidate the key physical processes involved in TC development.

2. Data and Methods

2.1. CloudSat Measurements

CloudSat is equipped with a lidar and cloud profiling radar to retrieve vertical profiles of cloud condensate. The vertical distributions of liquid and ice cloud effective radii and water contents along with ancillary temperature and humidity profiles from the European Centre for Medium-range Weather Forecasts analyses are used to initialize a broadband radiative flux model. The CloudSat 2B-FLXHR algorithm (L'Ecuyer et al., 2008) is used to produce a vertically resolved radiative flux and heating rate data set that is, consistent with observed reflectivities from CloudSat radar and lidar retrievals. Further details of the algorithm and flux products are described extensively in L'Ecuyer et al. (2008). The CloudSat Tropical Cyclone Data set (CSTC) provides a subset of CloudSat overpasses that have observed TCs over the past 15 years (Tourville et al., 2015; Wu & Soden, 2017). This study used measurements of radiative fluxes from version 2B-FLXHR P2_R04 from 2006 to 2015, to create composites for TCs.

2.2. CERES Measurements

The CERES project provides satellite-based observations of the earth's radiation budget and clouds (Doelling et al., 2013, 2016; Wielicki et al., 1996). It uses measurements of radiation from CERES instruments and auxiliaries of cloud properties from other satellites. The CERES instrument measures the radiation at the top of the atmosphere (TOA) through three channels, and is part of the NASA's Earth Observing System, flying on several satellites including the Tropical Rainfall Measuring Mission and the Moderate Resolution Imaging Spectroradiometer. The version of the data used in this study is the "synoptic TOA and surface fluxes and clouds" (SYN1deg-1Hour), which uses a radiative transfer model in combination with measurements of radiative fluxes, cloud properties, and aerosols from geostationary satellites to complement the data. The horizontal resolution is one-degree latitude/longitude, and the time interval is one hour.

We use the cloud radiative effect (CRE), defined as the difference between the clear sky and total sky radiative fluxes, to examine the effect of cloud radiative heating on the development of TCs. Specifically,

we consider the radiative heating from clouds within the atmospheric column, which is referred to as the Atmospheric Cloud Radiative Effect (ACRE). The ACRE is defined as the radiative flux convergence in the atmosphere due to clouds:

$$\text{ACRE} = (R_{\text{TOA}} - R_{\text{SFC}})_{\text{total}} - (R_{\text{TOA}} - R_{\text{SFC}})_{\text{clear}} \quad (1)$$

in which R_{TOA} and R_{SFC} represent the radiative flux at the top of the atmosphere and surface, respectively. The subscripts total and clear indicate total sky and clear sky conditions, respectively (Harrop & Hartmann, 2016; Hartmann et al., 1986).

2.3. Tropical Cyclone Genesis Archive

We use the tropical cyclone genesis archive of Cossuth et al. (2013) to determine whether TDs developed into tropical storms or hurricanes, hereafter referred to as TCs. Cossuth et al. (2013) used subjective Dvorak analyses to create tropical cyclogenesis climatology for every TD in the North Atlantic and North Eastern Pacific from 2000 to 2010. The Dvorak technique uses satellite measurements to quantify TC intensity from cloud growth and dissipation patterns (Dvorak, 1975, 1984). Cossuth et al. (2013) modified the technique to subjectively progress through steps from identifying the system in satellite imagery to determining the current intensity (CI) of convective systems. The CI number ranges from 1.0 to 8.0 with an interval of 0.5. Operationally, the National Hurricane Center requires a CI number of 2.0 to categorize the convective system as a TC. In this study, if a TD (CI < 2.0) grows to TC intensity (CI ≥ 2.0) after 24 h, we defined it as a developing TD. If a TD doesn't reach TC category after 24 h, we defined it as a non-developing TD. We also compared intensifying TCs with weakening TCs. The definition of intensifying/weakening TCs is if the CI number increases/decreases after 6 h. Complete details related to tropical cyclone genesis archive are available from Cossuth et al. (2013).

2.4. WRF Simulations

The advanced WRF model version 3.9.1 (Skamarock et al., 2008) is adopted to perform a series of sensitivity experiments. For these experiments, the horizontal resolution is 6 km with 540 × 540 horizontal grid points and 60 vertical levels. This configuration permits TC-environment interactions, which are considered to be crucial processes in the development of tropical convective systems, without the distortion from nested domains. The microphysical parameterization scheme is the 6-class single-moment scheme WSM6 (Hong & Lim, 2006), and the longwave and shortwave radiative parameterization is the rapid radiative transfer model for GCMs (RRTMG) (Iacono et al., 2008).

Two sets of simulations are executed to examine the effect of cloud-radiative interactions on TCs: a control simulation (CTL) and a parallel simulation that uses the spatially homogenized longwave radiative heating profiles (HOM_RA). The CTL maintains regular radiative processes, while HOM_RA prescribes the same profile of longwave radiative heating for the entire domain, which is derived from the spatial and temporal average of the control simulation with the same configuration. An ensemble of simulations is performed with both configurations by changing initial vortex intensity (7, 10, and 13 m/s at $z = 3.8$ km), the strength of vertical wind shear (difference between 200 and 850 hPa; 4, 6, 8, 10, and 12 m/s), and sea surface temperature (SST; 27 and 28°C). The point downscaling method of Nolan (2011) is adopted to specify the uniform background wind shear that is, nearly constant in time and space throughout the simulations. The initial vortex is a modified Rankine vortex, with the maximum wind at the radius of 150 km and the height of 3 km.

2.5. Budget Analysis

MSE is conserved during the moist adiabatic processes, and is a combination of internal, potential, and latent energy:

$$h = c_p T + gz + L_v q_v \quad (2)$$

where h is the MSE, L_v is the latent heat of evaporation, q_v is the vapor mixing ratio, and the other terms are the same as the conventional use in meteorology. Convection can redistribute MSE in the vertical but

cannot change column integrated MSE (CIMSE). Convective activity tends to increase as CIMSE increases (Raymond et al., 2009; Wing & Emanuel, 2014). Therefore, CIMSE is ideal for examining pathways of energy sources/sinks for convective systems. Previous studies have shown that the spatial variance of CIMSE is strongly correlated to the strength of the convective system within the domain (Wing & Cronin, 2016; Wing & Emanuel, 2014). We start with the budget equation for CIMSE, \hat{h} :

$$\frac{\partial \hat{h}}{\partial t} = \text{SEF} + \text{NetSW} + \text{NetLW} - \nabla_h \cdot \widehat{u\hat{h}} \quad (3)$$

where SEF is the surface enthalpy flux including latent and sensible heat flux, NetSW and NetLW are the radiative convergence in the atmospheric column for shortwave and longwave, respectively. The \hat{x} notion represents a density-weighted vertical integral from the surface to the top of the atmosphere. We subtract the horizontal mean of Equation 3 from the original Equation 3 and multiply the results by \hat{h}' , the anomaly of CIMSE, to obtain Equation 4:

$$\frac{1}{2} \frac{\partial \hat{h}'^2}{\partial t} = \hat{h}' \text{SEF}' + \hat{h}' \text{Net SW}' + \hat{h}' \text{Net LW}' - \hat{h}' \nabla_h \cdot \widehat{u\hat{h}'} \quad (4)$$

The x' notation indicates an anomaly from the horizontal mean. $\hat{h}' \nabla_h \cdot \widehat{u\hat{h}'}$ is the horizontal divergence of the CIMSE (not calculated in this study). The terms $\hat{h}' \text{SEF}'$, $\hat{h}' \text{Net SW}'$, $\hat{h}' \text{Net LW}'$ represent the correlations of \hat{h}' with its source and sink terms, which are surface enthalpy flux, and shortwave and longwave convergence in the atmospheric column, respectively.

3. Results

3.1. Satellite Measurements

We create composites of ACRE for outgoing longwave at the top of the atmosphere from CloudSat measurements for four intensity categories of TCs: tropical depression, tropical storm, category 1-2, and category 3-5 TCs, based on their current intensity and subsequent intensity change (Wu & Soden, 2017). Figure 1 shows that intensifying TCs, on average, have stronger ACRE than weakening TCs within 500 km of the TC center, except for category 3-5 TCs whose signal is unclear. The difference in ACRE between intensifying and weakening TCs is greater closer to the center. The greater ACRE in intensifying TCs is consistent with modeling studies which demonstrated that convective regions receive greater ACRE (Dudhia, 1989; Miller & Frank, 1993; Xu & Randall, 1995). Previous studies also suggested that the contrast of ACRE between the convective area and the environment plays a key role in convective organization (Bretherton et al., 2005; Muller & Held, 2012; Wing & Emanuel, 2014; Wing et al., 2017). Therefore, it is of interest to expand our domain to a broader area.

Since the CSTC data set only provides CloudSat observations within 500 km of the TC, whose coverage is only within the broad TC area, we adopt the CERES data set to examine how ACRE is distributed within the TC area and its environment. CERES measurements of radiative fluxes are used to create composites of ACRE for intensifying and weakening TCs based on 6-h intensity change. Each measurement is composited after subtracting its areal mean. For both intensifying and weakening TCs, the positive ACRE is concentrated within ~ 5 -degree latitude/longitude of the TC center (Figure 2a). The strength of ACRE increases and the area with strong ACRE of 60 W/m^2 expands as TC intensity becomes stronger. In addition, a greater ACRE occurs at the upper-right corner of TC, which might be evidence of the asymmetry induced by wind shear, though the composites don't rotate the measurements to the same direction of the wind shear.

To examine the impact of ACRE on TC development, Figure 2a shows the difference in ACRE between intensifying and weakening TCs. The areal mean ACRE within 5-degree latitude/longitude is $\sim 7 \text{ W/m}^2$ greater in intensifying TCs compared with weakening TCs, except for category 3-5 TCs whose difference is only about 2 W/m^2 . In contrast, the value in the area surrounding TCs is mostly negative to zero. The spatial contrast in ACRE is consistent with previous modeling studies related to convective self-aggregation which suggested that the contrast in radiative heating between the convective region and its environment plays a crucial role in nurturing the development of tropical convective systems (Wing & Emanuel, 2014; Wing & Cronin, 2016).

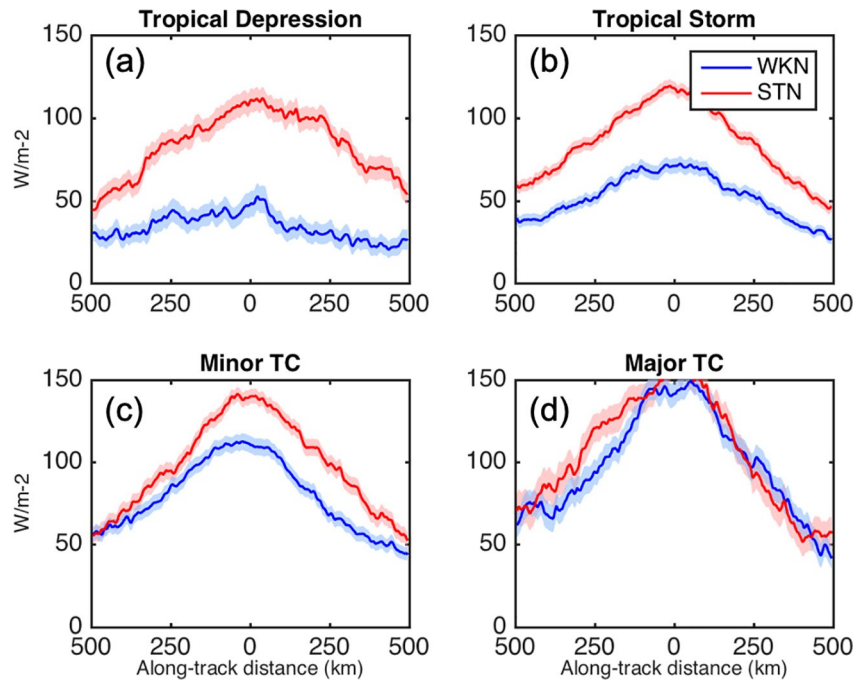


Figure 1. Observations of Atmospheric Cloud Radiative Effect of longwave radiative fluxes from CloudSat for intensifying and weakening tropical cyclones (TCs). Four panel represents different intensity categories: (a) tropical depression, (b) tropical storm, (c) category 1-2, and (d) category 3-5 TCs. Red line is intensifying TCs, and blue line is weakening TCs. Shadings are standard error. X-axis is the along-track distance to the zero point. Y-axis is CRE in W/m^{-2} .

To further examine how radiative heating contributes to the development of TCs, we perform a budget analysis of CIMSE to quantify the contribution from net longwave fluxes to the increase of energy in TCs using Equation 4. Previous studies performed the budget analysis for CIMSE to explore the important pathways that strengthen tropical convective systems (Wing & Cronin, 2016; Wing & Emanuel, 2014; Wing et al., 2016). However, it can be difficult to compute CIMSE from observations due to the lack of necessary measurements. Theoretical studies have suggested that the anomaly of CIMSE is dominated by column-integrated latent energy (i.e., water vapor), because the temperature gradient is small relative to the gradient of water vapor in the tropics (Raymond et al., 2009). Therefore, we utilize latent energy ($L_v \hat{q}_v$) from CERES measurements to replace CIMSE (\hat{h}) and perform the budget analysis using Equation 4. Latent energy is computed as the latent heat of evaporation multiplying column water vapor from the CERES data set. The contribution from radiative heating to the development of TCs can be disclosed through examining $\hat{h}' \text{Net LW}'$ (the third term on the right-hand side of Equation 4), which is termed as the anomaly of latent energy multiplying the anomaly of longwave radiation convergence within the atmosphere.

We create composites of $\hat{h}' \text{Net LW}'$ for intensifying and weakening TCs to examine the impact of radiative heating on the development of TCs (Figure 2b). The composites show that both intensifying and weakening TCs receive positive contributions from the net longwave radiative flux in the entire domain, with contributions about $500 \text{ kJ/m}^2 \cdot \text{kW/m}^2$ within the convective area. The positive value here indicates the positive feedbacks between CIMSE and net longwave radiative flux, which means high (low) CIMSE will get greater (smaller) because of anomalously high (low) longwave radiative flux convergence. This means that convective activity becomes stronger in the TC area and gets weaker in the environment. We further calculate their differences by subtracting weakening from intensifying TCs. For all intensity categories, contributions of net longwave radiative flux within convective regions are about twice as strong in intensifying TCs, while areas outside convective regions demonstrate negative to small positive values, except for category 3-5 TCs whose signal is unclear. A greater $\hat{h}' \text{Net LW}'$ within the TC area in intensifying TCs implies a stronger contribution from longwave radiation. We repeat the same analysis for shortwave radiative fluxes. The contribution from shortwave radiative fluxes is almost uniformly distributed across the domain,

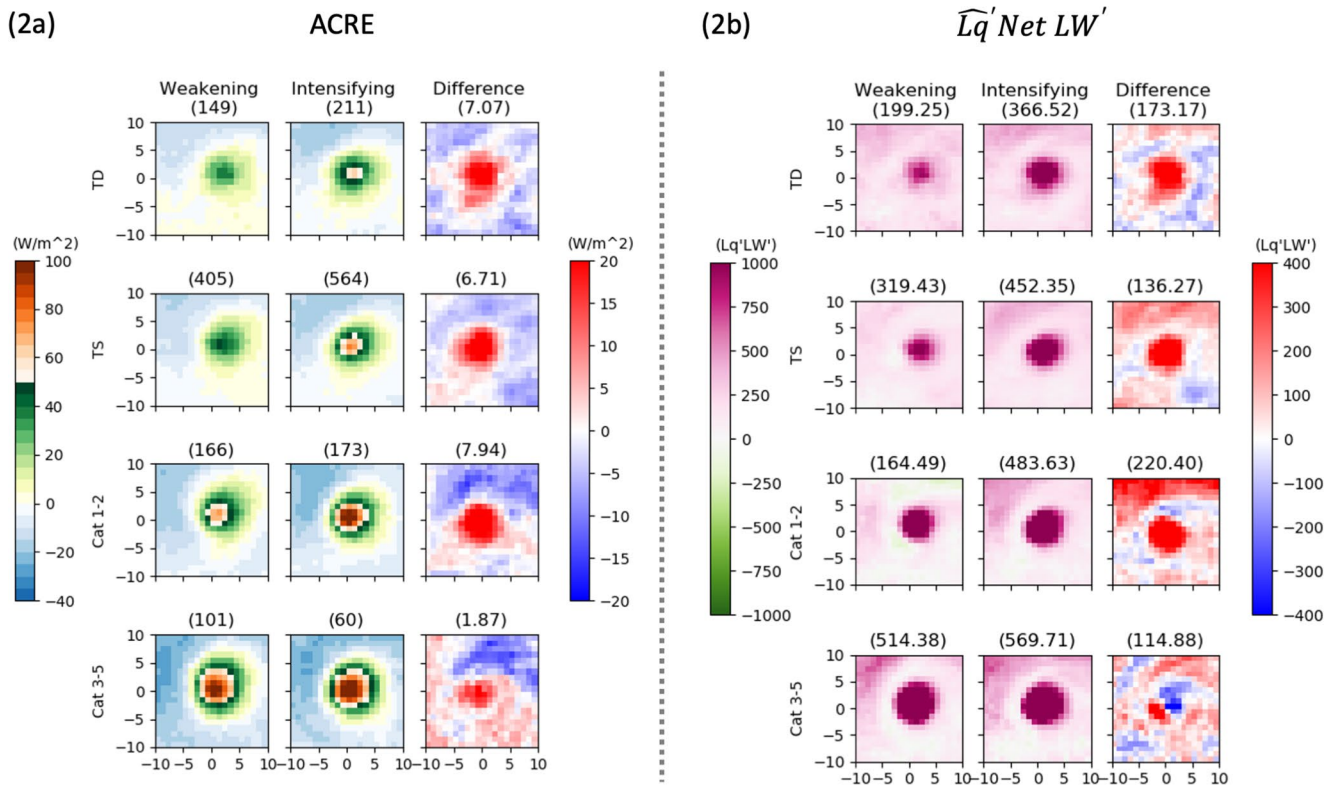


Figure 2. Observational composites from Clouds and the Earth’s Radiant Energy System measurements of (a) Atmospheric Cloud Radiative Effect and (b) $\widehat{h}'Net LW'$ for weakening tropical cyclone (TC), intensifying TC, and the difference between intensifying and weakening TCs as a function of intensity category. The x - and y -axis are longitude and latitude, respectively, in degrees. Numbers in intensifying and weakening columns in (a) are number of cases and (b) are the areal mean within 5 degree of latitude/longitude. Values in the difference column are the areal mean of their differences within 5 degree of latitude/longitude.

indicating that shortwave may only provide limited assistance to TC intensification (Figure S1). A greater contribution from longwave radiation to intensifying TCs seen in CERES measurements supports previous modeling studies that radiation is one of primary factors in influencing the evolution of TC intensity (Fovell et al., 2016; Melhauser & Zhang, 2014; Muller & Romps, 2018).

As radiative heating has been shown to be clearly related to the development of TCs, radiative heating may also play a crucial role in influencing TC genesis, when the primary and secondary circulations of convective systems are still immature. To investigate this, we create composites of ACRE for developing and non-developing TDs. Developing TDs are defined as those that intensify to a TC within 24 h. Composites show that developing TDs have stronger ACRE within the convective area than non-developing TDs (Figure S2). Within 5-degree latitude/longitude of the circulation center, the averaged ACRE in developing TDs is $\sim 6.5 W/m^2$ greater than that in non-developing TDs, while it is $\sim 2.5 W/m^2$ less than non-developing TDs outside the convective area (Figure 3a), consistent with the results for TC intensification. Furthermore, we extend the forecasting time from 24-h to 120-h with a 24-h interval to examine how early the signal of the enhanced ACRE occurs prior to TC genesis. The clear signal of the enhanced ACRE in the TC area and the suppressed ACRE in the environment can still be observed 72 h prior to TC genesis (Figure 3a). Even beyond the 72-h lead time, the developing TDs still have stronger ACRE around the circulation center (Figure 3a). We also examine the contribution from longwave radiative fluxes to TC genesis using the budget analysis and find results consistent with those for TC intensification (Figure 3b). That is, developing TDs have stronger contributions from longwave radiative fluxes within 5-degree latitude/longitude of the circulation center than non-developing TDs. The results of using CERES measurements demonstrate a clear difference in ACRE between developing and non-developing TDs in the convective area and the contribution from longwave radiative flux to the development of TCs, consistent with previous modeling studies which demonstrated that removing radiative heating may inhibit TC genesis (Carstens & Wing, 2020; Smith et al., 2020).

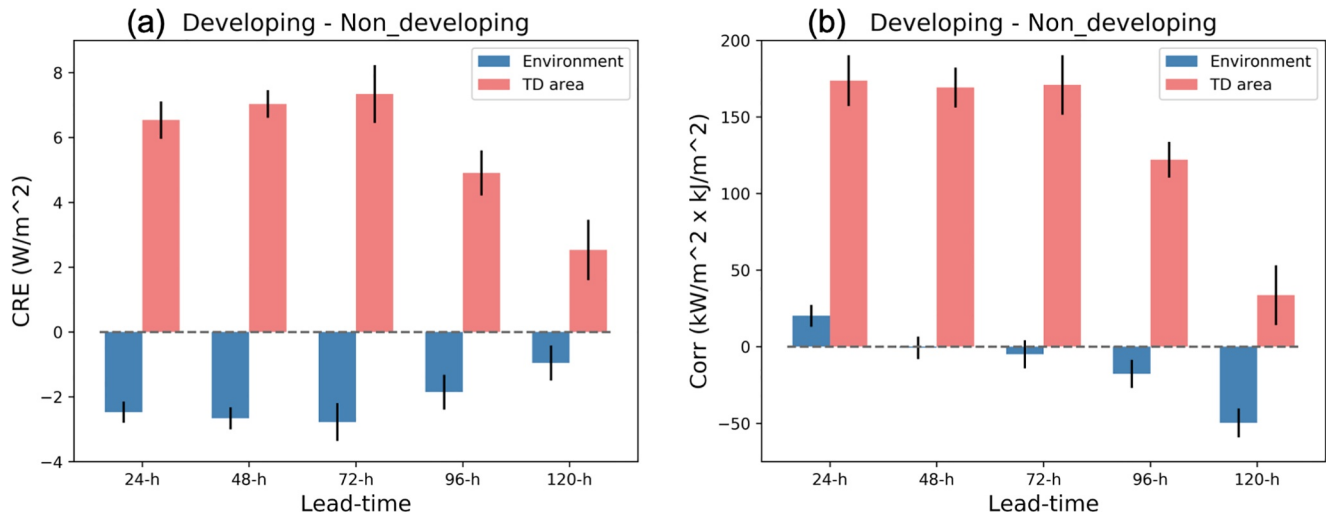


Figure 3. Observational composites of the areal-mean difference between developing and non-developing Tropical Depressions (TDs) of (a) Atmospheric Cloud Radiative Effect, (b) $\hat{h}'\text{Net LW}'$ from Clouds and the Earth's Radiant Energy System measurements. Red bars depict the areal mean within 5-degree latitude and longitude of the circulation center, referred to as the TD area, and blue bars depict the areal mean between 5-10° away from the circulation center, referred to as the TD environment. The black vertical lines represent one standard error from the areal mean. Different pairs represent different lead-time from 24-h to 120-h with a 24-h interval.

3.2. Model Simulations

Because the enhanced ACRE in developing TDs might be a response to the intensification rather than a cause of it, we use model sensitivity experiments to isolate the influence of ACRE on TC genesis. To examine the importance of the ACRE on the likelihood of TC genesis, we perform two sets of ensemble simulations, CTL and HOM_RA, with different environmental shear, SST and initial vortex intensities (7, 10, and 13 m/s). Overall, the number of TC genesis in CTL exceeds that in HOM_RA (Table S1). For a weak initial vortex (Figure 4a), most of the HOM_RA cases don't lead to TC genesis. Whereas, in CTL, only two out of 12 simulations don't undergo TC genesis due, partly, to the detrimental effect from high wind shear. For medium initial vortex intensity (Figure 4b), more vortices in HOM_RA achieve TC genesis, but the impact of homogenizing longwave radiative fluxes is to slow down intensification rates and to weaken the final vortex intensity. For a strong initial vortex (Figure 4c), only two of HOM_RA simulations don't achieve TC genesis, and the time for the rest of HOM_RA to reach TC genesis is much closer to the time in CTL, compared with weak and medium initial vortex cases. Regardless, HOM_RA still shows much slower intensification rates than those in control simulations. Accordingly, simulations in HOM_RA show less likelihood of TC genesis and slower intensification rates, indicating that removing cloud-radiative interactions suppresses TC development. The higher percentage of TC genesis events in CTL is consistent with previous modeling studies which suggested that cloud-radiative interactions play a crucial role in promoting tropical cyclogenesis (Carstens & Wing, 2020; Muller & Romps, 2018; Smith et al., 2020; Yang & Tan, 2020).

Next, we examine the evolution of the spatial variance of CIMSE (\hat{h}^2) and perform the budget analysis described in (Equation 4) to better understand the physical processes responsible for cyclogenesis. In each simulation, \hat{h}^2 increases with time (Figure 4d), and the evolution is similar to TC intensity as \hat{h}^2 is highly related to the strength of tropical convective systems (Wing & Cronin, 2016; Wing & Emanuel, 2014). The sharp gain of \hat{h}^2 in the first 24 h is due to the model spinup. After the first day, the growth rate of CTL is consistently faster than that in HOM_RA, and the evolution of CTL and HOM_RA diverges on the second day. The time of the divergence in the evolution suggests that the radiative feedbacks influence TC development from the earliest stages.

Because we substitute CIMSE with latent energy in the observational analysis, it is of interest to examine the viability of this method by comparing \hat{h}^2 with the spatial variance of latent energy in model simulations (Figure S3). Their values and evolution are highly similar, and their differences are only one-tenth of their

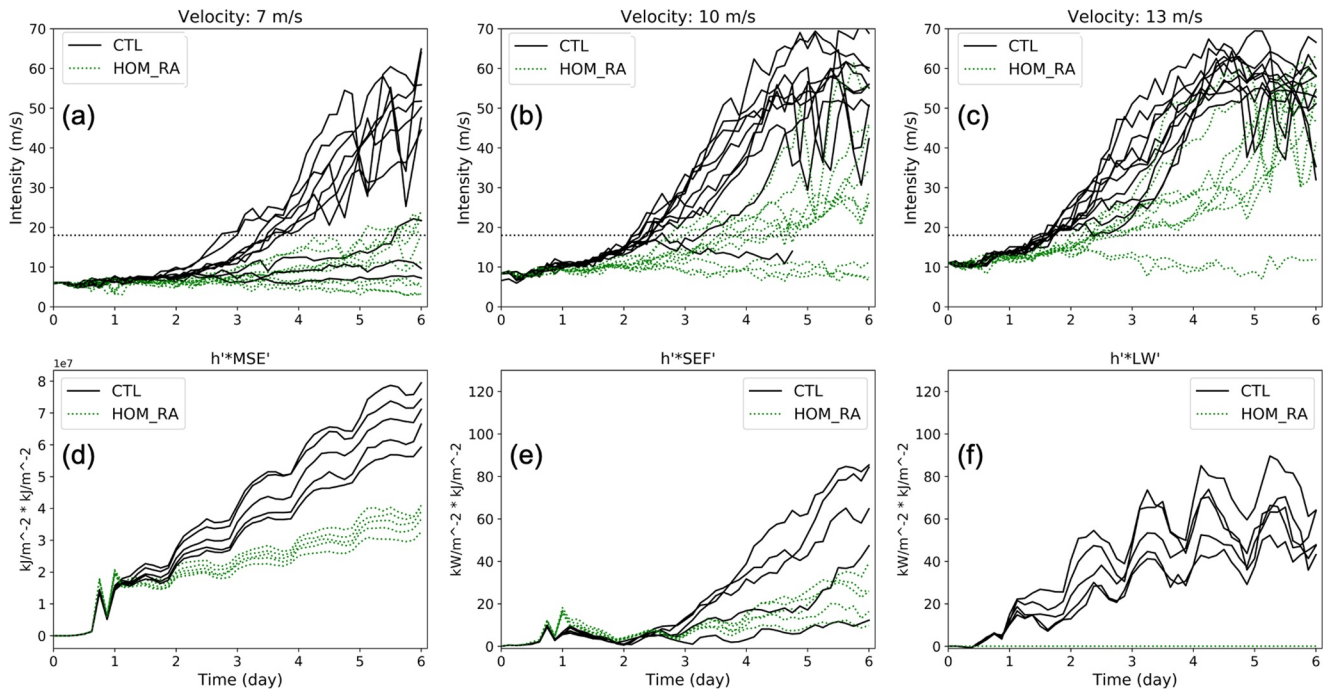


Figure 4. Model simulations of storm development for two different radiative heating experiments. The upper row, (a), (b), and (c), are the evolution of vortex intensity (m/s) for control simulation (CTL) (black) and HOM_RA (green dashed). The x-axis represents the simulation time in hour, and y-axis is vortex intensity in m/s. The initial vortex intensity is (a) 7 m/s, (b) 10 m/s, and (c) 13 m/s. The lower row, (d), (e), and (f) depicts the budget analysis of the spatial variance of column integrated moist static energy (CIMSE) for the weak initial vortex set (7 m/s) with sea surface temperature of 27°C, (d) is for the spatial variance of CIMSE, (e) is for surface enthalpy flux term, and (f) is for longwave radiative flux term. Black solid lines are CTL simulations and green dashed lines are HOM_RA simulations. The x-axis is simulation time in day, and y-axis is the spatial covariance between CIMSE and associated terms (left to right panels: CIMSE in $\text{kJ/m}^2 \cdot \text{kJ/m}^2$, surface enthalpy and longwave radiative flux in $\text{kJ/m}^2 \cdot \text{kW/m}^2$).

values, supporting the feasibility of using latent energy to represent CIMSE in the aforementioned satellite-based analysis.

To examine the contribution from the relevant physical processes toward the increase of spatial variance of CIMSE, we conduct a budget analysis for \hat{h}^2 , focusing on the contributions of surface enthalpy flux and longwave radiative flux, the first term ($\hat{h}'\text{SEF}'$) and third term ($\hat{h}'\text{Net LW}'$) on the right-hand side of Equation 4. Both terms show the similar magnitude of contribution to the increase of \hat{h}^2 , but their importance to increasing \hat{h}^2 is greater for different stages of development. For $\hat{h}'\text{SEF}'$, the value remains low and is almost identical between CTL and HOM_RA for the first two days (Figure 4e), while a clear difference appears at the beginning of the third day, in which $\hat{h}'\text{SEF}'$ in CTL rises sharply. For $\hat{h}'\text{Net LW}'$, HOM_RA is zero throughout the simulation, because the LW heating profiles are uniformly prescribed in the simulation (Figure 4f). Whereas, in CTL simulations, this term increases steadily while also showing diurnal oscillations. In CTL, the time when $\hat{h}'\text{Net LW}'$ increases significantly is one day earlier than the diverging time of \hat{h}^2 , suggesting that the net longwave radiative flux is the main contributor to the increase of \hat{h}^2 at the early stage of TCs. The leading contribution from longwave radiation to the increase of CIMSE within the circulation center at the early stage of simulations indicates that longwave radiation may be the primary factor in regulating TC genesis. This conclusion is consistent with previous modeling studies which suggested that longwave radiation is the leading contributor for tropical convective systems at their early stage (Carstens & Wing, 2020; Muller & Romps, 2018; Smith et al., 2020; Wing & Cronin, 2016; Wing & Emanuel, 2014).

4. Summary

This study examined the role of cloud-radiative interactions in the development of TCs using satellite-based retrievals of radiative fluxes and a small ensemble of WRF simulations. We found that TCs and TDs with enhanced ACRE tend to intensify in the future, especially for those with weak intensity. Furthermore, these greater ACRE and stronger cloud-radiative interactions found in developing TDs and TCs occur in the convective regions, suggesting the importance of radiation in facilitating the development of TCs. To verify the crucial role of cloud-radiative interactions in TC genesis, we conducted two sets of sensitivity experiments using different distributions of longwave radiative fluxes. Numerical simulations show that after uniformly prescribing longwave radiative fluxes, the occurrence of TC genesis is greatly reduced, especially for those simulations with weaker initial vortices. The reason for the reduced occurrence is due to the lack of cloud-radiative interactions as shown in the CIMSE budget analysis. According to both satellite-based and model-based analyses, cloud-radiative interactions promote tropical cyclogenesis. More analyses related to examining the physical processes that transport energy into TDs are required to elucidate the pivotal role of radiation in TC genesis.

Data Availability Statement

CloudSat overpasses were downloaded directly from CloudSat Tropical Cyclone Overpass data set (<https://adelaide.cira.colostate.edu/tc/>). CERES data were downloaded directly from CERES Data Product on NOAA website (<https://ceres.larc.nasa.gov/data/>). IBTrACS can be downloaded from the NOAA website (<https://www.ncdc.noaa.gov/ibtracs/>). WRF simulations were simulated using WRF3.9.1, which were downloaded from UCAR website (https://www2.mmm.ucar.edu/wrf/users/download/get_sources.html), and the initial configurations for a control simulation can be downloaded from the University of Miami Library (https://scholarship.miami.edu/discovery/fulldisplay?context=L&vid=01UOML_INST:ResearchRepository&search_scope=Research&tab=Research&docid=alma991031606061502976). Tropical cyclone genesis data is downloaded from the Tropical cyclone genesis archive website (<http://moe.met.fsu.edu/~jcosuth/genesis/>). Data is available through Cossuth et al. (2013).

Acknowledgment

This research was supported by NASA Awards 80NSSC18K1032, NNXW16AP19G and NOAA Award NA18OAR4310421.

References

- Bretherton, C. S., Blossey, P. N., & Khairoutdinov, M. (2005). An energy-balance analysis of deep convective self-aggregation above uniform SST. *Journal of the Atmospheric Sciences*, *62*, 4273–4292. <https://doi.org/10.1175/jas3614.1>
- Bu, Y. P., Fovell, R. G., & Corbosiero, K. L. (2014). Influence of cloud-radiative forcing on tropical cyclone structure. *Journal of the Atmospheric Sciences*, *71*, 1644–1662. <https://doi.org/10.1175/JAS-D-13-0265.1>
- Carstens, J. D., & Wing, A. A. (2020). Tropical cyclogenesis from self-aggregated convection in numerical simulations of rotating radiative-convective equilibrium. *Journal of Advances in Modeling Earth Systems*, *12*, e2019MS002020. <https://doi.org/10.1029/2019ms002020>
- Cossuth, J. H., Knabb, R. D., Brown, D. P., & Hart, R. E. (2013). Tropical cyclone formation guidance using pregenesis Dvorak climatology. Part I: Operational forecasting and predictive potential. *Weather and Forecasting*, *28*, 100–118. <https://doi.org/10.1175/WAF-D-12-00073.1>
- DeMaria, M., Sampson, C. R., Knaff, J. A., & Musgrave, K. D. (2014). Is tropical cyclone intensity guidance improving? *Bulletin of the American Meteorological Society*, *95*, 387–398. <https://doi.org/10.1175/BAMS-D-12-00240.1>
- Doelling, D. R., Haney, C. O., Scarino, B. R., Gopalan, A., & Bhatt, R. (2016). Improvements to the geostationary visible imager ray-matching calibration algorithm for CERES edition 4. *Journal of Atmospheric and Oceanic Technology*, *33*, 2679–2698. <https://doi.org/10.1175/JTECH-D-16-0113.1>
- Doelling, D. R., Loeb, N. G., Keyes, D. F., Nordeen, M. L., Morstad, D., Nguyen, C., et al. (2013). Geostationary enhanced temporal interpolation for CERES flux products. *Journal of Atmospheric and Oceanic Technology*, *30*(6), 1072–1090. <https://doi.org/10.1175/jtech-d-12-00136.1>
- Dudhia, J. (1989). Numerical study of convection observed during the winter monsoon experiment using a mesoscale two-dimensional model. *Journal of the Atmospheric Sciences*, *46*, 3077–3107. [https://doi.org/10.1175/1520-0469\(1989\)046<3077:NSOCOD>2.0.CO;2](https://doi.org/10.1175/1520-0469(1989)046<3077:NSOCOD>2.0.CO;2)
- Dunion, J. P., Thorncroft, C. D., & Velden, C. S. (2014). The tropical cyclone diurnal cycle of mature hurricanes. *Monthly Weather Review*, *142*, 3900–3919. <https://doi.org/10.1175/MWR-D-13-00191.1>
- Dvorak, V. F. (1975). Tropical cyclone intensity analysis and forecasting from satellite imagery. *Monthly Weather Review*, *103*, 420–430. [https://doi.org/10.1175/1520-0493\(1975\)103<0420:TCIAAF>2.0.CO;2](https://doi.org/10.1175/1520-0493(1975)103<0420:TCIAAF>2.0.CO;2)
- Dvorak, V. F. (1984). *Tropical cyclone intensity analysis using satellite data*. NOAA Tech. Rep (Vol. 11, p. 47). NESDIS.
- Fovell, R. G., Bu, Y. P., Corbosiero, K. L., Tung, W., Cao, Y., Kuo, H.-C., et al. (2016). Influence of cloud microphysics and radiation on tropical cyclone structure and motion. *Multiscale convection-coupled systems in the tropics: A tribute to Dr. Michio Yanai, Meteorological Monographs* (Vol. 56). American Meteorological Society.
- Harpop, B. E., & Hartmann, D. L. (2016). The role of cloud radiative heating within the atmosphere on the high cloud amount and top-of-atmosphere cloud radiative effect. *Journal of Advances in Modeling Earth Systems*, *8*, 1391–1410. <https://doi.org/10.1002/2016MS000670>
- Hartmann, D. L., Ramanathan, V., Berroir, A., & Hunt, G. E. (1986). Earth radiation budget data and climate research. *Reviews of Geophysics*, *24*(2), 439–468. <https://doi.org/10.1029/RG024i002p00439>

- Hong, S.-Y., & Lim, J.-O. J. (2006). The WRF Single-Moment 6-Class Microphysics Scheme (WSM6). *Journal of the Korean Meteorological Society*, 42, 129–151.
- Iacono, M. J., Delamere, J. S., Mlawer, E. J., Shephard, M. W., Clough, S. A., & Collins, W. D. (2008). Radiative forcing by long-lived greenhouse gases: Calculations with the AER radiative transfer models. *Journal of Geophysical Research*, 113, D13103. <https://doi.org/10.1029/2008JD009944>
- L'Ecuyer, T. S., Wood, N. B., Haladay, T., Stephens, G. L., & Stackhouse, P. W. (2008). Impact of clouds on atmospheric heating based on the R04 CloudSat fluxes and heating rates data set. *Journal of Geophysical Research*, 113, D00A15. <https://doi.org/10.1029/2008JD009951>
- Melhauser, C., & Zhang, F. (2014). Diurnal radiation cycle impact on the pregenesis environment of Hurricane Karl (2010). *Journal of the Atmospheric Sciences*, 71, 1241–1259. <https://doi.org/10.1175/JAS-D-13-0116.1>
- Miller, R. A., & Frank, W. M. (1993). Radiative forcing of simulated tropical cloud clusters. *Monthly Weather Review*, 121, 482–498. [https://doi.org/10.1175/1520-0493\(1993\)121<0482:RFOTC.2.0.CO;2](https://doi.org/10.1175/1520-0493(1993)121<0482:RFOTC.2.0.CO;2)
- Muller, C., & Held, I. M. (2012). Detailed investigation of the self-aggregation of convection in cloud-resolving simulations. *Journal of the Atmospheric Sciences*, 69, 2551–2565. <https://doi.org/10.1175/jas-d-11-0257.1>
- Muller, C. J., & Romps, D. M. (2018). Acceleration of tropical cyclogenesis by self-aggregation feedbacks. *Proceedings of the National Academy of Sciences of the United States of America*, 115, 2930–2935. <https://doi.org/10.1073/pnas.1719967115>
- Nolan, D. S. (2011). Evaluating environmental favorableness for tropical cyclone development with the method of point-downscaling. *Journal of Advances in Modeling Earth Systems*, 3, M08001. <https://doi.org/10.1029/2011MS000063>
- Nolan, D. S., Moon, Y., & Stern, D. P. (2007). Tropical cyclone intensification from asymmetric convection: Energetics and efficiency. *Journal of the Atmospheric Sciences*, 64, 3377–3405. <https://doi.org/10.1175/jas3988.1>
- Nolan, D. S., Rappin, E. D., & Emanuel, K. A. (2007). Tropical cyclogenesis sensitivity to environmental parameters in radiative–convective equilibrium. *Quarterly Journal of the Royal Meteorological Society*, 133, 2085–2107. <https://doi.org/10.1002/qj.170>
- Raymond, D. J., Sessions, S. L., Sobel, A. H., & Fuchs, Z. (2009). The mechanics of gross moist stability. *Journal of Advances in Modeling Earth Systems*, 1, 9. <https://doi.org/10.3894/JAMES.2009.1.9>
- Ruppert, J. H., Wing, A. A., Tang, X., & Duran, E. L. (2020). The critical role of cloud–infrared radiation feedback in tropical cyclone development. *Proceedings of the National Academy of Sciences of the United States of America*, 117, 27884–27892. <https://doi.org/10.1073/pnas.2013584117>
- Simon, A., Penny, A. B., DeMaria, M., Franklin, J. L., Pasch, R. J., Rappaport, E. N., & Zelinsky, D. A. (2018). A description of the real-time HFIP Corrected Consensus Approach (HCCA) for tropical cyclone track and intensity guidance. *Weather and Forecasting*, 33, 37–57. <https://doi.org/10.1175/WAF-D-17-0068.1>
- Skamarock, W. C., Klemp, J. B., Dudhia, J., Gill, D. O., Barker, D. M., Duda, M. G., et al. (2008). *A description of the Advanced Research WRF version 3*. NCAR Tech. Note NCAR/TN-4751STR, 113 pp., <https://doi.org/10.5065/D68S4MVH>
- Smith, W. P., Nicholls, M. E., & Pielke, R. A. (2020). The role of radiation in accelerating tropical cyclogenesis in idealized simulations. *Journal of the Atmospheric Sciences*, 77, 1261–1277. <https://doi.org/10.1175/JAS-D-19-0044.1>
- Tourville, N., Stephens, G., DeMaria, M., & Vane, D. (2015). Remote sensing of tropical cyclones: Observations from CloudSat and A-Train profilers. *Bulletin of the American Meteorological Society*, 96, 609–622. <https://doi.org/10.1175/BAMS-D-13-00282.1>
- Wang, Y., Davis, C. A., & Huang, Y. (2019). Dynamics of lower-tropospheric vorticity in idealized simulations of tropical cyclone formation. *Journal of the Atmospheric Sciences*, 76, 707–727. <https://doi.org/10.1175/jas-d-18-0219.1>
- Wielicki, B. A., Barkstrom, B. R., Harrison, E. F., Lee, R. B., Smith, G. L., & Cooper, J. E. (1996). Clouds and the Earth's Radiant Energy System (CERES): An Earth observing system experiment. *Bulletin of the American Meteorological Society*, 77, 853–868. [https://doi.org/10.1175/1520-0477\(1996\)077<0853:CATERE>2.0.CO;2](https://doi.org/10.1175/1520-0477(1996)077<0853:CATERE>2.0.CO;2)
- Wing, A. A., Camargo, S. J., & Sobel, A. H. (2016). Role of radiative–convective feedbacks in spontaneous tropical cyclogenesis in idealized numerical simulations. *Journal of the Atmospheric Sciences*, 73, 2633–2642. <https://doi.org/10.1175/jas-d-15-0380.1>
- Wing, A. A., & Cronin, T. W. (2016). Self-aggregation of convection in long channel geometry. *Quarterly Journal of the Royal Meteorological Society*, 142, 1–15. <https://doi.org/10.1002/qj.2628>
- Wing, A. A., Emanuel, K., Holloway, C. E., & Muller, C. (2017). *Convective self-aggregation in numerical simulations: A review, shallow clouds, water vapor, circulation, and climate sensitivity* (pp. 1–25). Cham: Springer. https://doi.org/10.1007/978-3-319-77273-8_1
- Wing, A. A., & Emanuel, K. A. (2014). Physical mechanisms controlling self-aggregation of convection in idealized numerical modeling simulations. *Journal of Advances in Modeling Earth Systems*, 6, 59–74. <https://doi.org/10.1002/2013ms000269>
- Wu, S., & Soden, B. J. (2017). Signatures of tropical cyclone intensification in satellite measurements of ice and liquid water content. *Monthly Weather Review*, 145, 4081–4091. <https://doi.org/10.1175/MWR-D-17-0046.1>
- Wu, S., Soden, B. J., Miyamoto, Y., Nolan, D. S., & Buehler, S. A. (2021). Using satellite observations to evaluate the relationships between ice condensate, latent heat release, and tropical cyclone intensification in a mesoscale model. *Monthly Weather Review*, 149(1), 113–129. <https://doi.org/10.1175/MWR-D-19-0348.1>
- Wu, S.-N., Soden, B. J., & Alaka, G. J. (2020). Ice water content as a precursor to tropical cyclone rapid intensification. *Geophysical Research Letters*, 47, e2020GL089669. <https://doi.org/10.1029/2020gl089669>
- Xu, K.-M., & Randall, D. A. (1995). Impact of interactive radiative transfer on the macroscopic behavior of cumulus ensembles. Part II: Mechanisms for cloud–radiation interactions. *Journal of the Atmospheric Sciences*, 52, 800–817. [https://doi.org/10.1175/1520-0469\(1995\)052<0800:IOIRTO.2.0.CO;2](https://doi.org/10.1175/1520-0469(1995)052<0800:IOIRTO.2.0.CO;2)
- Yang, B., & Tan, Z.-M. (2020). Interactive radiation accelerates the intensification of the midlevel vortex for tropical cyclogenesis. *Journal of the Atmospheric Sciences*, 77, 4051–4065. <https://doi.org/10.1175/JAS-D-20-0094.1>
- Zhang, B., Soden, B. J., Vecchi, G. A., & Yang, W. (2021). The role of radiative interactions in tropical cyclone development under realistic boundary conditions. *Journal of Climate*, 34(6), 2079–2091. <https://doi.org/10.1175/jcli-d-20-0574.1>